

GYROSCOPIC FEATHERING MOMENTS AND THE ‘BELL STABILISER BAR’ ON HELICOPTER ROTORS

I. A. Simons (Visiting lecturer)⁺
A. N. Modha (Research student)

School of Engineering Sciences, Aerospace Engineering, University of Southampton, SO17 1BJ. U.K.

Abstract

Rotor blade feathering moments caused by the gyroscopic forces acting during helicopter pitching and rolling motions are identified. The consequent blade elastic feathering motion incurred by these moments are shown to give rise to blade flapping which reduces the pitch/roll cross-coupling due to the aerodynamic effects of pitch and roll motions. For blades of low feathering stiffness this reduction is considerable. Inclusion of this effect into rotor analysis can account for much of the difference between calculated cross-coupling and observed flight behaviour. This suggests that ‘dynamic inflow’ or other effects introduced to explain these discrepancies, should be re-evaluated.

The ‘Bell Bar’ rotor system is reviewed and it is shown that the stabiliser bar may be considered as an extension of the rotor blade, and gyroscopic feathering moments are a fundamental reason for its operation as a beneficial influence on helicopter flight behaviour.

Notation

a_0	blade aerofoil lift-curve slope = $dC_L/d\alpha$
c	blade chord
C_L	lift coefficient
C_T	rotor thrust coefficient = $T / \frac{1}{2} \rho (\Omega R)^2 \pi R^2$
D_θ	damping about feathering axis
$D_{\theta \text{ crit}}$	= $2\lambda_\theta$; critical value of damping about feathering axis
I_β	blade inertia about flapping hinge
I_θ	blade inertia about feathering hinge
K_β	spring stiffness about flapping hinge
K_θ	spring stiffness about feathering axis
$L(r)$	blade lift on at radius r , per unit length
$M_{\text{ext}}(r)$	‘extraneous’ pitching moment on blade at radius r , per unit length
n_β	blade flap inertia no. = ratio of aerodynamic to inertial flap forces, (= Lock no./ 8)
p, q	aircraft roll rate (+ve port up), pitch rate (+ve nose up)
p^*, q^*	aircraft roll, pitch rate normalised by Ω
r	radius of blade element
R	rotor tip radius
S_β	blade stiffness number = ratio of elastic to aerodynamic flap forces

t	time
T	rotor thrust
v_i	induced velocity at rotor disc
$\alpha(r)$	incidence of blade aerofoil section
$\beta(\psi)$	= $\beta_0 + \beta_{1s} \sin \psi + \beta_{1c} \cos \psi$; blade flap angle
ζ_θ	= $D_\theta / D_{\theta \text{ crit}}$, pitch (feather) damping ratio
θ	= $\theta_{\text{applied}} + \theta_{\text{tw}}$; pitch (feather) angle of blade
θ_{applied}	= $\theta_0 + \theta_{1s} \sin \psi + \theta_{1c} \cos \psi$; pitch applied to blade via control system
θ_{tw}	= $\theta_{\text{tw}0} + \theta_{\text{tw}1s} \sin \psi + \theta_{\text{tw}1c} \cos \psi$; blade elastic twist about feathering hinge
λ_β	natural flapping frequency ratio of blade
λ_θ	natural feathering frequency ratio of blade
λ_i	induced velocity normalised by tip-speed ΩR
μ	tip-speed ratio, flight velocity/ ΩR
ρ	air density
ψ	= Ωt , blade azimuth, $\psi = 0$ at rear of disc
Ω	rotor rotational speed

GYROSCOPIC FEATHERING MOMENTS

Introduction

The helicopter with its edgewise rotor is a peculiarly asymmetric aircraft, characterised by cross-coupled responses to control and flight state variations, and this makes the prediction of flight manoeuvres especially difficult. One area of particular concern is the coupling between the longitudinal and lateral motions when the helicopter is subjected to pitch and roll rates, as has been noted by Prouty (Ref. 1) who reported large differences between theory and flight behaviour of the Apache helicopter.

The reasons for this are still not fully resolved but one explanation that has been invoked – and particularly favoured over the past two decades – is that of ‘dynamic inflow’ where the induced velocity at the rotor disc is varied as a function of flight state parameters and their rates of change, including pitch and roll angular velocities (e.g. Refs 2,3).

⁺ Presented at the European Rotorcraft Forum, Bristol England, September 17-20, 2002. Copyright©2002 by I. A. Simons and A. N. Modha. All rights reserved.

However, there is another physical phenomenon at work on rotors which explains, and to a seemingly large extent, such cross-coupling discrepancies. It is the feathering moment induced by the gyroscopic forces acting on the distributed chord-wise mass of the blade. These gyroscopic feathering moments very rarely, if ever, appear in the analyses of rotor behaviour. It seems that helicopterists have suffered from a collective oversight over the years and either never appreciated that this inertial moment exists, or perhaps dismissed it as very small and therefore of no consequence. This is certainly not the case however as the moment, although small, is proportional to blade feathering inertia and therefore is potentially a source of considerable elastic feathering.

This note retains gyroscopic feathering moments in an analysis of blade flapping and shows that, on rotors with typical blade feathering flexibility, cross-coupling predictions better reflect the observed flight behaviour.

Finally, the analysis is used to provide a description of the functioning of the 'Bell Bar' rotor system.

Rotor Theoretical Model

The theoretical examination of the rotor presented here follows 'classical simple' analysis as found in many texts such as Newman (Ref 4) and Bramwell (Ref 5).

The physical model used here is of a rotor having rigid, untwisted, constant chord blades with

- flapping hinge at the centre of rotation, with spring restraint about the hinge which accounts for the effect of an offset flap hinge or a 'flexible hinge',
- feathering hinge inboard, feathering axis along the blade 1/4 chord which is also the aerodynamic centre of the blade aerofoil section,
- conventional swash-plate control system with some flexibility in the pitch-link arms, which allows an 'elastic' feathering displacement additional to any applied control,
- chord-wise centre-of-mass at the 1/4 chord; constant mass distribution along blade,
- zero thickness, i.e. flat in the chordwise direction.

The aerodynamic theory follows conventional practice with a constant lift-curve slope, uniform induced velocity over the rotor disc, and small angle assumptions.

The analysis is restricted to the first harmonic (1 per rotor revolution) quasi-steady blade response, as is usual in the traditional, simpler considerations of flight mechanical behaviour. Furthermore, for simplicity and clarity, the analysis is restricted to hover conditions although the principal results are almost unchanged in forward flight conditions.

Blade Flapping

The well-known equation defining the flapping motion of a rotor blade is

$$I_{\beta} \cdot \partial^2 \beta / \partial t^2 + (\Omega^2 I_{\beta} + K_{\beta}) \cdot \beta = \int L(r) \cdot r \, dr + I_{\beta} (2\Omega p \cdot \cos \psi - 2\Omega q \cdot \sin \psi) \quad -1$$

The last term defines the moment about the blade flap hinge due to the gyroscopic inertial force acting in the flapwise sense.

After defining blade lift in the usual manner, and some manipulation, the equation becomes,

$$\partial^2 \beta / \partial \psi^2 + n_{\beta} \cdot \partial \beta / \partial \psi + \lambda_{\beta}^2 \cdot \beta = n_{\beta} \cdot [\theta_0 + \theta_{1s} \sin \psi + \theta_{1c} \cos \psi + \theta_{tw} + p^* \sin \psi + q^* \cos \psi] + 2 (p^* \cdot \cos \psi - q^* \cdot \sin \psi) \quad -2$$

where $\lambda_{\beta}^2 = 1 + K_{\beta} / \Omega^2 I_{\beta}$ is the natural frequency ratio.

The p and q terms within the square brackets reflect the aerodynamic incidence at the blade induced by the pitch and roll motions, whereas the final p and q terms are due to the gyroscopic forces.

Assuming, for now, no blade dynamic twisting θ_{tw} , the solution of this equation is

$$\beta_{1s} = \{ +\theta_{1c} + \theta_{1s} S_{\beta} + p^* (2/n_{\beta} + S_{\beta}) + q^* (1 - 2S_{\beta}/n_{\beta}) \} / (1 + S_{\beta}^2)$$

$$\beta_{1c} = \{ -\theta_{1s} + \theta_{1c} S_{\beta} - p^* (1 - 2S_{\beta}/n_{\beta}) + q^* (2/n_{\beta} + S_{\beta}) \} / (1 + S_{\beta}^2) \quad -3$$

To illustrate these results consider $\lambda_{\beta} = 1$ (i.e. $S_{\beta} = 0$) – as for an articulated rotor with central flap hinge – and set $n_{\beta} = 1$ for simplicity.

$$\beta_{1s} = +\theta_{1c} + 2 \cdot p^* + q^*, \quad \beta_{1c} = -\theta_{1s} - p^* + 2 \cdot q^*, \quad -4$$

The flapping response to cyclic pitch may be expressed $\beta_{cyclic}(\psi + 90^\circ) = \theta_{cyclic}(\psi)$ i.e. the well-known result that flapping equals cyclic pitch but lags by 1/4 revolution. Flapping response to pitch rate may be expressed as $\beta(\psi)/q^* = \sqrt{5} \cdot \cos(\psi - 26^\circ)$ showing that the rotor disc tilts so as to oppose the pitch rate, but with a lag of nearly 1/12 revolution.

Blade Aeroelastic Twisting (Feathering)

In the simple rotor model used here the blade is rigid and aeroelastic twisting is represented by a pitching about the feathering hinge, possible because of flexibility in the control system. Note that this elastic twisting is additional to that applied via the controls.

The equation governing the twisting motion is

$$I_0 \cdot \partial^2 (\theta_{applied} + \theta_{tw}) / \partial t^2 + \Omega^2 I_0 \cdot (\theta_{applied} + \theta_{tw}) + K_0 \cdot \theta_{tw} = \int M_{ext}(r) \cdot dr - I_0 \cdot (2\Omega p \cdot \sin \psi + 2\Omega q \cdot \cos \psi) \quad -5$$

The second term, the ‘propeller moment’, is due to the centrifugal force (sometimes referred to as the tennis-racket effect) and has its origin in the blade chordwise mass distribution (Refs 4, 5).

The last term defines the feathering moment due to the gyroscopic forces acting on the distributed chordwise mass and is proportional to the blade feathering inertia. Although the existence of this moment has been noted in standard texts (e.g. Ref 5 p9) it appears to have been dismissed as very small and therefore of no consequence.

It is to be noted that this moment exists even when the chordwise centre-of-mass is on the feathering axis. A centre-of-mass offset gives rise to an additional feathering moment proportional to the total gyroscopic force (in the flap sense) multiplied by the offset.

M_{ext} indicates any other, undesirable ‘extraneous’ feathering moments such as aerodynamic moments and structural moments resulting from blade elastic deformations such as pitch/flap/lag coupling (Ref 6).

The elastic feathering equation can be manipulated to giveⁱ

$$\frac{\partial^2 \theta_{tw}}{\partial \psi^2} + \lambda_{\theta}^2 \cdot \theta_{tw} = \frac{1}{\Omega^2 I_0} \cdot \int M_{ext}(r) \cdot dr - 2 (p^* \cdot \sin \psi + q^* \cdot \cos \psi) \quad -6$$

where $\lambda_{\theta}^2 = 1 + K_{\theta} / \Omega^2 I_0$ is the natural frequency ratio.

As it is standard practice to design rotor blades such that the extraneous moments are as low as possible, it will be assumed that the ratio of such moments to inertial forces is very small,

$$\text{i.e. } \int M_{ext}(r) \cdot dr \ll \Omega^2 I_0 \quad -7$$

so that the twisting equation becomes

$$\frac{\partial^2 \theta_{tw}}{\partial \psi^2} + \lambda_{\theta}^2 \cdot \theta_{tw} = -2 (p^* \cdot \sin \psi + q^* \cdot \cos \psi) \quad -8$$

Note that there is no damping term but, in practice there is likely to be a little aerodynamic, structural or frictional damping present, sufficient to ensure stability.

The solution is

$$\theta_{tw1s} = -2 p^* / (\lambda_{\theta}^2 - 1), \quad \theta_{tw1c} = -2 q^* / (\lambda_{\theta}^2 - 1) \quad -10$$

Clearly, if the natural feathering frequency is low, blade twist in response to pitch and roll rates can be very considerable. [Note that the natural frequency must be greater than 1. A value of 1 is possible if there were no control system attached to the blade, as any control

ⁱ Note that, as the analysis is restricted to first harmonic variations only, $\frac{\partial^2 \theta_{applied}}{\partial \psi^2} + \theta_{applied} = 0$

linkages must have a stiffness which would ensure a natural feathering frequency greater than unity.]

Note that a roll (pitch) rate induces only a sine (cosine) twisting motion that, in turn, induces a cosine (sine) flapping response. Such flapping means that the rotor disc tilts in a pitch (roll) sense – that is a cross-coupling effect.

Coupled Blade Flapping and Feathering Motion

Now that the unconnected blade flapping and blade twisting behaviour has been reviewed the coupled behaviour can be investigated.

Equations (10) for cyclic twisting are substituted into equations (3) for flapping response to give expressions for blade flapping when twisting is included. As this leads to lengthy equations in the general case it is sensible to forgo this step and move on to a consideration of the results for specific values of S_{β} , λ_{θ} that are of interest. For simplicity the flapping stiffness will be set to zero – i.e. $S_{\beta} = 0$ – throughout the following.

The solution is

$$\begin{aligned} \beta_{1s} &= p^* \cdot (2 / n_{\beta}) + q^* \cdot [1 - 2 / (\lambda_{\theta}^2 - 1)] \\ \beta_{1c} &= q^* \cdot (2 / n_{\beta}) - p^* \cdot [1 - 2 / (\lambda_{\theta}^2 - 1)] \end{aligned} \quad -11$$

It is clear that the twisting induced by the gyroscopic feathering moments reduces the cross-coupling effect produced by the aerodynamic effects of roll and pitch rates. For typical values of $n_{\beta} = 1$ and $\lambda_{\theta} = 3.5$ the cross coupling terms are reduced by some 16%. At a lower feathering frequency of $\lambda_{\theta} = 2.5$ the reduction is a substantial 32%.

Simons (Ref 7) has shown that this effect explains phenomena noticed during flight tests in the early 1970’s with the Westland hingeless-rotor Research Scout helicopter (Ref 9)ⁱⁱ which were alike those noted by Prouty (Ref 1). As mentioned before, the effect, if not the existence, of gyroscopic feathering moments seems to be generally overlookedⁱⁱⁱ and other mechanisms have been sought to explain the reduction in cross-coupling.

Results

Calculations, with the theory outlined above, of the effect of gyroscopic feathering moments on rotor blade flapping response to pitch and roll rates are illustrated in figures 1 and 2. The results are displayed as variations with feathering frequency of rotor derivatives with respect to pitch and roll rates.

ⁱⁱ Reference 9 does not discuss this particular topic.

ⁱⁱⁱ Padfield (Ref 8) draws attention to the findings of reference 7 but does not investigate any further.

Figure 1 refers to an articulated rotor with blades hinged at the centre line – i.e. $\lambda_\beta = 1$, $S_\beta = 0$ – and a typical blade inertia of $n_\beta = 1$. The reduction in the cross-coupling terms β_{1s}/q^* and β_{1c}/p^* is seen to be considerable at low feathering frequencies λ_θ , reflecting equation (11) above.

Figure 2 refers to a rotor with a flap frequency ratio of $\lambda_\beta = 1.092$ ($S_\beta = 0.1925$) which is typical of hingeless rotor systems such as the MBB Bo105 and the Westland Lynx. Now, as a consequence of the reduced phase lag between cyclic pitch and flap response, the cross-coupling rate derivatives are somewhat less than for the articulated rotor. Indeed, at low feathering frequencies these terms approach zero – i.e. no cross-coupling effect. There is also some variation in the derivative of rotor thrust with roll rate which is not shown in the figures.

Although these results clearly indicate the cross-coupling in the rotor flapping behaviour, the effect on helicopter behaviour must take into account the inertias of the aircraft about its pitch and roll axes. As the ratio of pitch to roll inertia is typically 3-4, the magnitude of roll/pitch angular accelerations associated with unit lateral and longitudinal disc tilts is of the same order. Thus the roll coupling instigated by a pitch rate is considerably higher than the pitch coupling induced by a roll rate.

A simple 6-degree-of-freedom model of a helicopter has been used to calculate response to a pilot cyclic pitch input to demand a nose-down pitch manoeuvre in the hover. For this study a generic helicopter model is used, with a rotor as described earlier. The fuselage is assumed to have only an aerodynamic drag force, there is no tailplane or fin and an actuator disc is used for the tail rotor. The helicopter centre-of-mass is 21.23% of main rotor radius below the hub and on the shaft line. Pitch and roll radii of gyration are 30% and 13.3% of radius respectively. No stabilisation system is included in the model. The equations of motion in classical derivative form are used to calculate the helicopter motions.

Figures 3 and 4 show the pitch and roll rate time histories following application of a 1 degree cyclic pitch control in the nose-down sense, for an articulated rotor and a hingeless rotor. The decrease in secondary roll motion, resulting from the gyroscopic feathering moments on blades of low feathering frequency, is well illustrated, especially in the case of the stiffer rotor, and is certainly comparable to the observations of ref. 1.

APPLICATION TO THE BELL ROTOR SYSTEM

Introduction

It is a query of most people, when they study the helicopter, as to why the rotor does not act like a gyroscope and provide stability to the helicopter rather than burden the aircraft with a natural instability. Closer inspection shows that this instability is traceable to the rotor's aeroelastic behaviour – to the interaction between the airloads acting on the blades and their dynamic motion. In the early years of helicopter development many individuals spent considerable effort trying to find design features which would restore to the rotor the 'lost' gyroscope features, and thus improve the stability and control of the helicopter.

The 'Bell' stabiliser bar was one of the few design solutions that actually did provide some improvements and has stood the test of time; – it has been used on most of the Bell range of helicopters over the years. A similar device, also stemming from the early days, is the Hughes 'paddle' bar and, in later years, Lockheed introduced the 'gyro-controlled' rotor which might be viewed as a much refined version of the original stabiliser bar

A new look at the Bell rotor system is now undertaken, taking into account the gyroscopic feathering moments discussed above.

Model of Bell Rotor System

The Bell stabiliser bar, in essence, is a heavy bar attached to the main rotor shaft below the rotor hub (usually), and having a freedom to 'flap'. About its flapping hinge is a viscous damper. The bar, aligned with its radius at right angles to the blade radius, is mechanically connected to the feathering hinge of the rotor blades such that bar flapping and blade feathering is equal^{iv} in the absence of any pilot control inputs.

Pilot's controls, via a swash-plate, are attached to the linkages between the bar and blades allowing the application of collective and cyclic pitch. The controls effectively change the length of the bar-blade linkage; at once per revolution in the case of cyclic pitch application.

The 'bar flap + blade pitch' freedom (which here is termed 'twist' to correspond to the previous analysis) is independent of the pilot-applied pitch angles. Moreover this twist freedom comes with no spring restraint (i.e. no mechanical stiffness) within the linkage system so that the twist natural frequency is once per revolution – i.e. $\lambda_\theta = 1$. [The bar alone, with no flap spring, has a natural flap frequency of 1; the blade alone, having no pitch axis spring, has a natural feathering frequency of 1; and so the combined 'bar flap

^{iv} In practice the connecting linkage may be such that bar flap and blade feathering might not be identical but in some fixed relationship. This difference is not crucial to the present analysis and is ignored.

+ blade pitch' freedom also retains a natural frequency of unity.] Note also that the damper only operates on the twist motion and does not affect the applied pitch.

Figure 5 illustrates, in schematic form, the Bell rotor system.

Clearly, if the bar flap and blade twist motions are identical then the bar can be ignored as a separate entity, and simply considered as an addition to the blade. Physically one can visualise the stabiliser bar as moved from its low position up to the hub and then attached directly to the blade – it is now obvious that the bar provides an increase in the blade chordwise dimension and mass, and hence feathering inertia. The bar's flap damper is then seen to act as a damper about the blade feathering hinge.

Pilot controls, as described above, can still be connected into the pitch links between damper and blade. However, the controls may also be taken from the swash-plate directly to the 'earthed' side of the viscous damper which will still allow cyclic pitch to be imposed. [As the blade has a natural pitch frequency of 1/revolution, a pilot cyclic control input will lead to a cyclic feathering such that there is no damper displacement.] Of course this layout cannot accommodate collective pitch control and an additional mechanism would be required such as a separate control linkage led up through the rotor shaft. Figure 6 illustrates this equivalent Bell rotor system.

For the present purposes this control layout is adequate as it emulates the Bell rotor system although, undoubtedly, better control architectures could be devised.

The blade flapping and twisting behaviour of this equivalent rotor can now be analysed in the same manner as done previously for a conventional rotor.

Blade Aeroelastic Twisting with Damping

The effect of adding damping around the feathering hinge is now considered. As before the extraneous pitching moments are assumed small, but now a damping moment of $D_{\theta} \partial \theta_{tw} / \partial t$ is added. Although, as has been pointed out, the natural frequency of the twist motion is $\lambda_{\theta} = 1$, it is kept initially as a variable in the analysis.

The previous equations (5,6) governing twisting become

$$\begin{aligned} I_{\theta} \partial^2 \theta_{tw} / \partial t^2 + D_{\theta} \partial \theta_{tw} / \partial t + (\Omega^2 I_{\theta} + K_{\theta}) \theta_{tw} \\ = - I_{\theta} (2\Omega p \cdot \sin \psi + 2\Omega q \cdot \cos \psi) \\ \partial^2 \theta_{tw} / \partial \psi^2 + (D_{\theta} / \Omega I_{\theta}) \partial \theta_{tw} / \partial \psi + \lambda_{\theta}^2 \theta_{tw} \\ = - 2 (p^* \cdot \sin \psi + q^* \cdot \cos \psi) \end{aligned} \quad -13$$

Now expressing the damping term in terms of critical damping gives

$$\begin{aligned} \partial^2 \theta_{tw} / \partial \psi^2 + \zeta_{\theta} \cdot 2\lambda_{\theta} \cdot \partial \theta_{tw} / \partial \psi + \lambda_{\theta}^2 \theta_{tw} \\ = - 2 (p^* \cdot \sin \psi + q^* \cdot \cos \psi) \end{aligned} \quad -14$$

where $\zeta_{\theta} = (D_{\theta} / D_{\theta \text{ crit}}) =$ damping ratio, and critical damping $D_{\theta \text{ crit}} = 2\Omega I_{\theta} \lambda_{\theta}$. which has the solution -15

$$\begin{aligned} \theta_{tw1s} = \\ \{-2 p^* \cdot (\lambda_{\theta}^2 - 1) - 2 q^* \cdot 2\lambda_{\theta} \zeta_{\theta}\} / \{(\lambda_{\theta}^2 - 1)^2 + (2\lambda_{\theta} \zeta_{\theta})^2\} \\ \theta_{tw1c} = \\ \{-2 q^* \cdot (\lambda_{\theta}^2 - 1) + 2 p^* \cdot 2\lambda_{\theta} \zeta_{\theta}\} / \{(\lambda_{\theta}^2 - 1)^2 + (2\lambda_{\theta} \zeta_{\theta})^2\} \end{aligned} \quad -16$$

The assumption made in the analysis, that $\int M_{ext}(r) \cdot dr \ll \Omega^2 I_{\theta}$ (equation 7), is now even more sensible as the total 'bar + blade' inertia is substantially higher than that of the blade alone. This is perhaps one of the most important aspects of the Bell rotor.

Now consider the case of a feathering natural frequency $\lambda_{\theta} = 1$, and non-zero damping $\zeta_{\theta} \neq 0$, which reflects the Bell rotor. The expressions for blade twist reduce to

$$\theta_{tw1s} = -q^* / \zeta_{\theta}, \quad \theta_{tw1c} = +p^* / \zeta_{\theta}. \quad -17$$

Note now that the gyroscopic feathering moments brought about by a roll (pitch) rate induce only a cosine (sine) twisting motion. Also the twisting is only affected by the feathering damping ratio – the stabiliser bar does not appear in the expressions, other than indirectly through the damping ratio.

Combined Flap and Feather Equations

Substituting the expressions for blade twist (17) into the flapping equation (3) gives

$$\begin{aligned} \beta_{1s} = +p^* \cdot [2/n_{\beta} + 1/\zeta_{\theta}] + q^* \\ \beta_{1c} = -p^* + q^* \cdot [2/n_{\beta} + 1/\zeta_{\theta}] \end{aligned} \quad -18$$

It is seen that the twisting caused by the gyroscopic feathering moments generated by a roll (pitch) rate induces a sine (cosine) flapping response – i.e. the rotor disc tilts in a roll (pitch) sense which is opposed to the aircraft motion – that is a positive damping effect. This effect adds to the damping produced by the gyroscopic flapping forces acting on the blades.

For a value of $n_{\beta} = 1$ and feathering damping equal to the critical value, i.e. $\zeta_{\theta} = 1$, the damping disc tilt is increased by 50%. Although cross-coupling is not reduced its value relative to the damping term is considerably lower which may provide some improvement in helicopter handling characteristics.

Equivalent Bell Rotor System Results

Calculations of blade flapping response to pitch and roll rates are illustrated in figure 7, which can be compared to figures 1, 2 for 'conventional' rotors. Results are shown for two values of the feathering damping ratio – 100% and 50% of critical. The substantial increase in the direct derivatives β_{1s}/p^* and β_{1c}/q^* compared to he conventional rotor is seen.

The response of a helicopter with this Bell rotor system to a nose-down pitch demand in the hover is depicted in figures 8 and 9 (cf. figures 3, 4). Results for both an articulated rotor and a hingeless rotor are shown. A considerable reduction in angular rates in both the demanded and off-axis directions, due to the higher rotor damping is evident.

Concluding Comments

The analysis presented has shown that

- on a conventional rotor the gyroscopic inertial feathering moments, acting on the blades when the rotor is rolling or pitching, induce a twist that gives rise to a disc tilt in the cross-coupling sense, but opposing that cross-coupling produced by the aerodynamic effects of rolling and pitching, and
- the magnitude of this twist increases as blade feathering natural frequency decreases, such that
- on rotors with blade flap frequency above 1/revolution, and a low feathering frequency of ~ 2.5 /revolution, the total cross-coupling may be substantially negated (or even reversed).

In view of these results it is recommended that

- gyroscopic feathering moments be included in all rotor analyses concerned with manoeuvring flight conditions,
- that any other mechanisms introduced to improve cross-coupling predictions, such as dynamic inflow models, be reviewed for applicability.

Further it has been shown that the stabiliser bar on Bell rotors can be considered as an addition to the blade feathering inertia and that

- removing stiffness about the feathering axis, so that the natural frequency ratio is unity,
- and adding viscous damping about the feathering axis,

changes the direction of disc tilt caused by gyroscopic feathering moments so that it opposes the pitch and roll rates and adds to the disc tilt produced by the gyroscopic flapping forces.

The merit of the Bell rotor system design is that it provides a mechanism for

- divorcing the conventional rotor blade pitch control system from an additional pitch freedom with natural frequency of 1/revolution,
- introducing viscous damping into the blade feathering system
- increasing the feathering inertia of the blades which reduces the effect of any undesired/extraneous pitching moments on the blades.

References

1. Prouty, R.W.; "The Case of the Cross-Coupling Mystery". Rotor and Wing International, June 1994
2. Pitt, D.M.; Peters, D.A.; "Rotor Dynamic Inflow Derivatives and Time Constants from Various Inflow Models". Paper 55, 9th European Rotorcraft Forum, Italy, Sept. 1983
3. Theodore, C. and Celi, R.; Prediction of the Off-Axis response to cyclic pitch using a manoeuvring free wake model. Proceedings of the 25TH European Rotorcraft Forum, Rome, Italy, Sept. 1999
4. Newman, S.J.; "The Foundations of Helicopter Flight". Edward Arnold 1994, ISBN 0-340-587024
5. Bramwell, A.R.S.; Done, G.T.S.; Balmford, D.E.H.; "Bramwell's Helicopter Dynamics". Butterworth Heinemann 2001, ISBN 0-7506-5075-3
6. Hansford, R.E.; Simons, I.A.; "Torsion-Flap-Lag Coupling on Helicopter Rotor Blades". Journal of the American Helicopter Society, October 1973
7. Simons, I.A.; "The Effect Of Gyroscopic Feathering Moments On Helicopter Rotor Manoeuvre Behaviour". Westland Helicopters Ltd., Research Paper 404, August 1971.
8. Padfield, G.D.; "Helicopter Flight Dynamics". Blackwell Science Ltd. 1996. ISBN 0-632-05607-X
9. Balmford, D.E.H.; "Ground and Flight test Experience with the Westland Scout Hingeless Rotor Helicopter" in Advanced Rotorcraft, Vol. 1 AGARD CP-121, 1973.

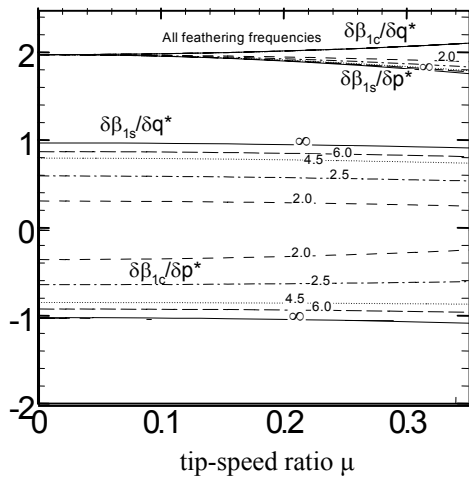


Figure 1. Effect of gyroscopic feathering moments on an articulated rotor ($\lambda_\beta=1$, $n_\beta=1$) - blade flapping response to cyclic control and to pitch and roll rates.

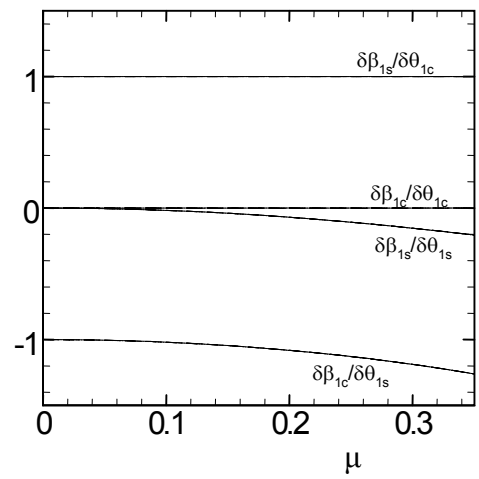


Figure 1 continued.

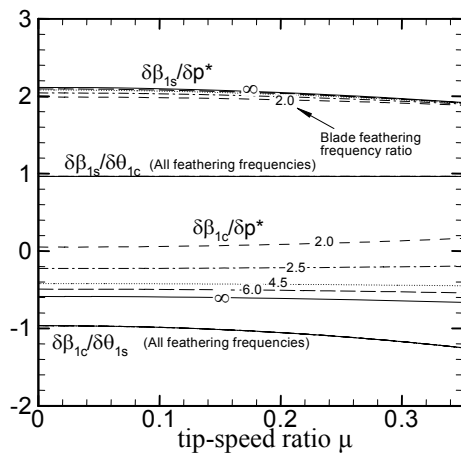


Figure 2. Effect of gyroscopic feathering moments on a hingeless rotor ($\lambda_\beta=1.092$, $n_\beta=1$) - blade flapping response to cyclic control and to pitch and roll rates.

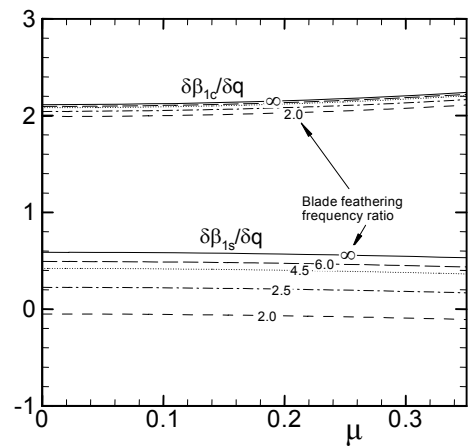


Figure 2 continued.

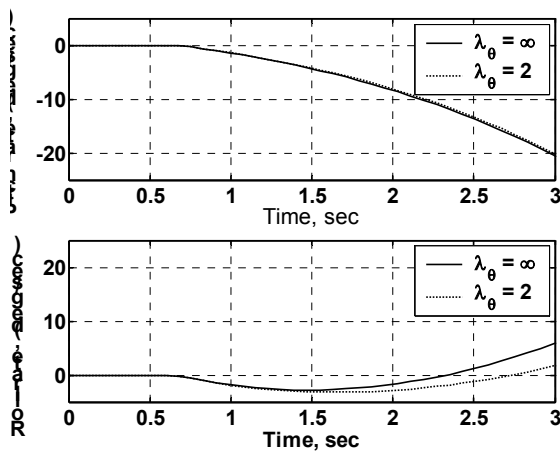


Figure 3. Effect of feathering stiffness on pitch and roll rate response to a step nose-down control input in hover, - articulated rotor helicopter ($\lambda_\beta=1$, $n_\beta=1$)

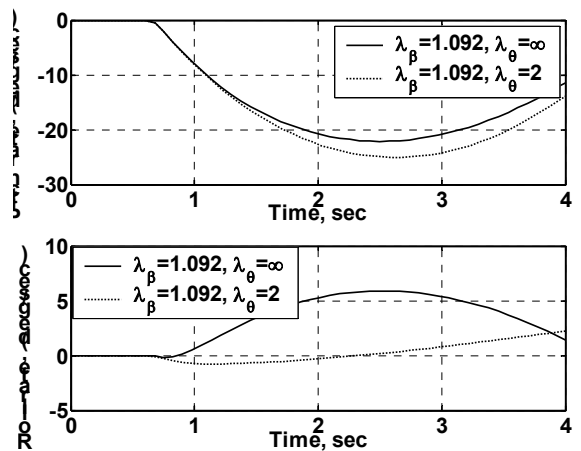


Figure 4. Effect of feathering stiffness on pitch and roll rate response to a nose-down cyclic step input in hover, - hingeless rotor helicopter ($\lambda_\beta=1.092$, $n_\beta=1$)

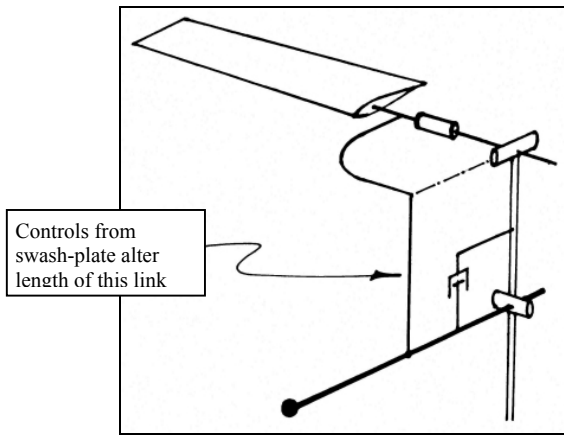


Figure 5. Bell rotor system configuration

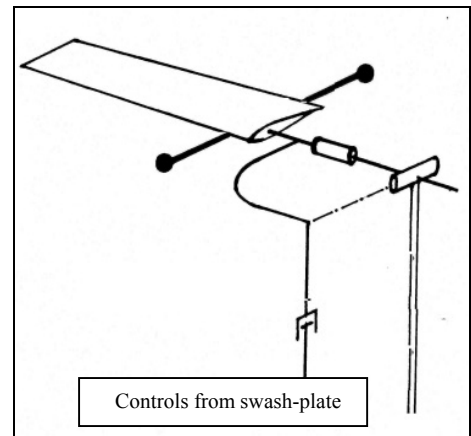


Figure 6. Equivalent Bell rotor configuration

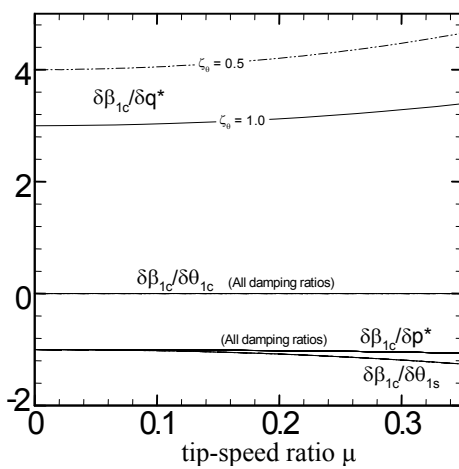


Figure 7. Equivalent Bell rotor system ($\lambda_\beta = 1, n_\beta = 1$) -blade flapping response to cyclic control and to pitch and roll rates.

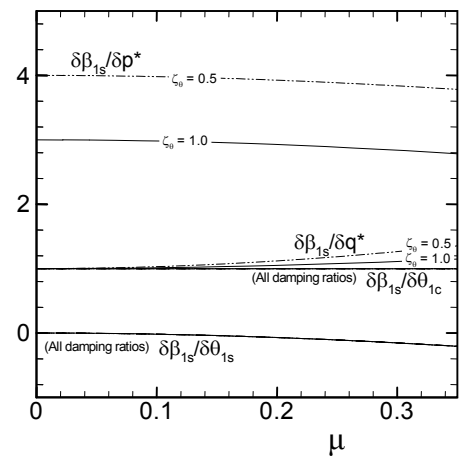


Figure 7 continued.

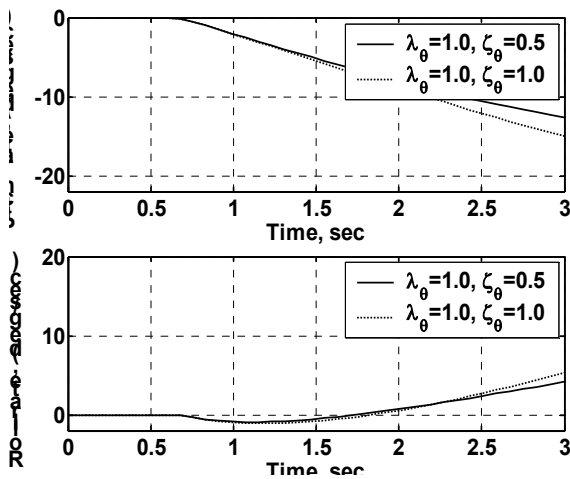


Figure 8. Pitch and roll rate response to a step nose-down control input in hover, - equivalent Bell rotor helicopter with articulated blade ($\lambda_\beta = 1, n_\beta = 1$)

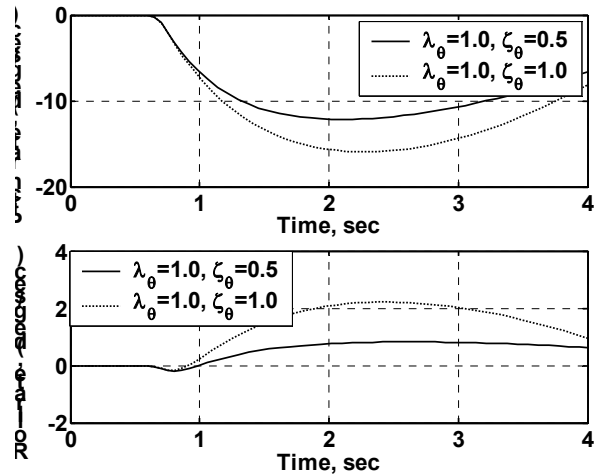


Figure 9. Pitch and roll rate response to a step nose-down control input in hover, - equivalent Bell rotor helicopter with hingeless blade ($\lambda_\beta = 1.092, n_\beta = 1$)